Green Chemistry

PAPER

View Article Online
View Journal | View Issue

Cite this: *Green Chem.*, 2025, **27**, 227

Electrochemical hydrogenation of alkenes over a nickel foam guided by life cycle, safety and toxicological assessments†

Pedro J. Tortajada, [a] Therese Kärnman, [b] Pablo Martínez-Pardo,[a] Charlotte Nilsson,[c] Hanna Holmquist, [b] Magnus J. Johansson[a,d] and Belén Martín-Matute *[a]

Received 17th June 2024,
Accepted 16th November 2024

DOI: 10.1039/d4gc02924k

rsc.li/greenchem

The electrochemical hydrogenation of enones and alkenes using commercial nickel foam and an aqueous acidic solution is presented. The reaction shows excellent selectivity in C=C *vs.* C=O reduction, with enhanced activity when using 7% of *n*BuOH as cosolvent. The method presents good applicability and recyclability properties, with more than 30 different substrates explored, and it can be recycled at least 15 times. Toxicological and screening life cycle assessments were used to identify potential "hot-spots" of environmental and human health impact during the development phase of the method, as well as to evaluate the performance of the electrochemical nickel method against the conventional use of Pd/C and H_2 gas.

Introduction

The hydrogenation of carbon–carbon double and triple bonds is a fundamental chemical reaction with important applications in the food, petrochemical, and pharmaceutical industries.[1–3] Traditionally, hydrogenation reactions use a metal catalyst, usually Pd or Pt, with hydrogen gas (H_2) as the reductant.[2] Rare metal catalysts are prominent in this field, thus their replacement by abundant metal catalysts, such as nickel offers a more sustainable alternative.[2,4,5] For example, catalysts such as RANEY® nickel or nickel oxide have been used extensively in hydrogenation reactions.[5–7]

The use of H_2 as the reductant gives excellent atom economy, but also presents major drawbacks: hydrogen gas is derived primarily from fossil resources, and it is also a hazardous material.[8–10] Apart from transfer hydrogenations using water as reductant,[11–14] one viable alternative is to use electrochemical water splitting that occurs during the hydrogen evolution reaction (HER) as source of hydrogen,[15,16] avoiding its transportation and manipulation.[17] Electrocatalysts are needed for HER, and these electrodes are usually dependent on platinum-group metals because of their low overpotential requirements.[18–20] However, the scarcity and high cost of platinum hinders their widespread application.[21–23] Nickel foams and their modified variants can provide a good balance between activity for the HER, recyclability, and safety.[24–26]

The electrochemical hydrogenation (ECH) of C–C multiple bonds have been achieved using diverse hydrogen sources, such as water, NH_4Cl, NH_3, or nBu_4NHSO_4.[27,28] Frequently, electrolytes such as nBu_4PF_6 and solvents such as MeCN or DMSO are used.[27,28] Replacing these solvents with water, which can also serve as the proton source, offers advantages in terms of safety and availability. Additionally, it allows for the use of widely available and abundant electrolytes like NaOH or H_2SO_4. ECH are vastly catalyzed by platinum-group metals.[17,27,28] Only a few examples have been reported using nickel foams; Zhang and colleagues demonstrated the semihydrogenation of terminal alkynes to alkenes using a selenium-functionalized nickel foam ($Ni_{0.85Se1-x}$) in a basic aqueous solution (Fig. 1a).[29] The reaction relies on the presence of selenium on the surface of the nickel foam for optimal catalytic activity. The authors highlighted that the efficiency of the ECH of alkynes into alkenes was attributed to the exceptional performance of $Ni_{0.85Se1-x}$ in the hydrogen evolution reaction. The Martín-Matute group described the selective semihydrogenation of terminal and of 1,2-disubstituted alkynes using an unfunctionalized commercially available nickel foam as an electrocatalyst in an acidic solution (Fig. 1b).[30] Control experiments revealed that electrochemically generated nickel

[a]*Department of Organic Chemistry, Stockholm University, 106 91 Stockholm, Sweden. E-mail: belen.martin.matute@su.se*
[b]*IVL Swedish Environmental Research Institute, 411 33 Gothenburg, Sweden*
[c]*RISE Research Institutes of Sweden, 151 36 Södertälje, Sweden*
[d]*Medicinal Chemistry, Research and Early Development, Cardiovascular, Renal and Metabolism (CVRM) Biopharmaceuticals R&D AstraZeneca, 431 50 Mölndal, Sweden*
† Electronic supplementary information (ESI) available. See DOI: https://doi.org/10.1039/d4gc02924k

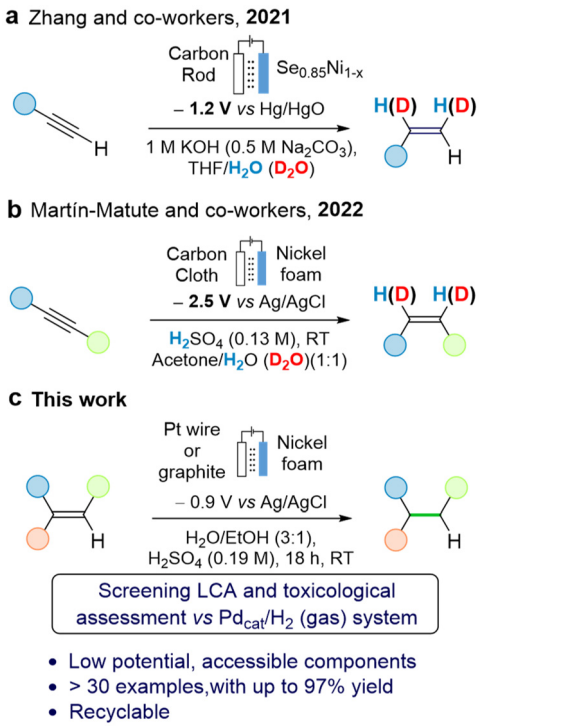

Fig. 1 (a and b) Strategies for the hydrogenation of alkynes using (functionalized) nickel foams under electrochemical conditions. (c) This work.

hydrides were the key species responsible for alkyne reduction, and that the produced H_2 *via* HER did not act as the reductant. The Zhang and Martín-Matute systems can both convert alkynes into alkenes very efficiently, but their use for the full reduction to saturated derivatives was not explored. A recent paper by Najafpour and coworkers described the ECH of styrene using nickel foam as both sacrificial anode and cathode in a single cell configuration. However, the high cell potential (3.4 V) limits its applicability.[31]

Here we present the use of nickel foam as readily available, abundant, and safe catalyst for the reduction of alkenes into saturated derivatives using water as the hydrogen source (Fig. 1c). Aiming at embracing the safe and sustainable by design concept,[32–37] a screening life-cycle assessment (LCA) was carried out alongside the method development, to assess the environmental impact of the new process. Carrying out LCA at the early stages of chemical process development presents important challenges, such as defining the functional unit, data availability, definition of system boundaries, and the fact that significant changes might take place when the reaction is scaled-up.[38,39] Our objectives are two-fold: (i) Developing a catalytic method using nickel for alkene hydrogenation guided by environmental and toxicological assessments that identifies areas of concern ("hotspots"); and (ii) Evaluating the environmental performance of the nickel foam system, including human toxicity indicators, as a catalytic alternative to the traditional method Pd/C and H_2 gas.[40,41]

Materials and methods

Electrochemical method

Nickel foam (1.6 × 10 × 20 mm, 95% porosity) was immersed in H_2SO_4 3 M and sonicated at room temperature for 10 min. The substrate was added to the cathode compartment in the H-cell (ESI, Fig. S1 and S2†), separated by a silica frit (G4) and loaded with 25 mL of electrolyte solution on each cell. The working electrode (nickel foam) was placed at 10 mm depth from the solution's surface. Platinum wire was used as counter electrode. Distance between electrodes was around 54 mm. Potentials were measured *vs.* a Ag/AgCl/KCl 3 M reference electrode. The electrolysis was conducted at controlled potential, using a GAMRY Interface E1010 or a Biologic VSP-3e potentiostat. No impedance compensation was employed. Unless otherwise stated, all experiments were carried out at room temperature and open to air. Faradaic Efficiency (FE) was determined as the fraction of current used in the hydrogenation of interest compared with the total current. See the ESI for further details (Section S1.2†).

Screening life cycle assessment

Screening LCA was used as the tool to provide insights on potential environmental and human health impacts and resource use for the hydrogenation.[42] The basis for assessment is the function provided by the product or service, described with the functional unit. The life cycle perspective employed is cradle-to-gate, which implies considerations of emissions and resource use from all activities in raw material acquisition and production of a substance, but not its use, as it is unspecified. Environmental impacts caused by the products after the hydrogenation reactions are excluded from the comparison, but further treatment of waste streams as generated in the production process were considered, albeit in a generic modelling approach, *e.g.* by inclusion of municipal solid waste treatment. The functional unit was set to 1.00 g of isolated product based on the lab scale on which this work was developed.

The life cycle inventory (LCI) data for the nickel foam method was collected from combining the 0.154 g scale reaction of 2-cylohexenone (**1b**) and the recyclability study (*vide infra*). The data for the Pd/C method was obtained from 1 g scale reactions of *p*-hydroxybenzylidene acetone (**1a**) and cylohexenone (**1b**) (*vide infra*). In the baseline scenario, an electricity grid mix for Sweden was used. In a theoretical future scenario grid mix for 2030 was modelled. Statistics from the International Energy Agency from 2018 was used to obtain electricity grid data for Sweden.[43] The system description of both methods can be found in the ESI (Section S4.1†).

The indicative results were calculated using the impact assessment model USEtox 2.12 for ecotoxicity and human toxicity impact categories and EF 3.0 for remaining impact categories, as implemented in GaBi (version 10.5.1.124, professional database [DB] version 2021.2).[44–46] Further details can be found in the ESI (Section S4†). In LCA all relevant potential impacts are to be covered, *i.e.* not only climate change but also *e.g.* toxicity, acidification and eutrophication,

which allows for quantitative assessment of potential problem shifting not only between life cycle stages but also between impact categories. The following impact categories were studied due to their anticipated relevance: acidification, climate change, eutrophication potential (freshwater and marine), resource use (mineral and metals), ecotoxicity and human toxicity (cancer and non-cancer).

Assessment of safety and toxicity

The identification of a series of physical safety hazards such as pyrophoricity, along with biological/toxicological hazards, relied on substance classifications, including hazard codes and statements, as per REACH and CLP notifications. It also considered whether the substance fell under harmonized classification and labelling (CLH).[47] When evaluating the risks stemming from biological hazards, exposure approximations were also taken into account.

The criteria for evaluating the hydrogenation methods relied on environmental, safety and toxicological performance. The economic value related to the processes is out of the scope of this study.

Results and discussion

At the outset of our studies, various reaction conditions were tested for the electrochemical reduction of *p*-hydroxy benzylidene acetone **1a** (Table 1). As H_2 production is a side reaction for this system, FE was used to determine the fraction of electrons involved in the target ECH, while also evaluating the extent of the HER side reaction. The commercially supplied nickel foam was first activated by sonication in H_2SO_4 (3 M aq.) for 10 min. This activation was carried out a single time on the commercially supplied foam, after purchasing. When the electrochemical reduction reaction of **1a** was carried out under the same conditions as in our previous study on the reduction of alkynes (*vide supra*, Fig. 1b),[30] namely a mixture 1 : 1 (v/v) of acetone and H_2SO_4 (0.5 M aq.), only a moderate yield of the product was obtained, and a very low FE was observed (Table 1, entry 1). This was not surprising, as these conditions were optimized for the selective semihydrogenation of alkynes to alkenes, and any further hydrogenation to form saturated derivatives occurred at much lower rates. The yield increased when MeOH was used as the organic cosolvent instead of acetone, although the FE of this reaction was low (Table 1, entry 2). By increasing the MeOH/H_2SO_4 ratio to 3 : 1 (v/v), the FE were improved; this also allowed us to decrease the applied potential to −0.9 V (Table 2, entries 3 and 4). Under these conditions a good yield of 78% was obtained, with a FE of 4%. The concentration of H_2SO_4 was lowered to 0.19 M, which provided a good yield of 77% (Table 1, entry 5).

A toxicological assessment identified significant health hazards related to the use of MeOH as an organic solvent. Once absorbed, its metabolism produces formic acid, a highly toxic compound that can cause organ damage, particularly to eye tissues.[48,49] Therefore, EtOH[50] was tested under otherwise identical reaction conditions (Table 1, entry 6), affording and increased yield of 89% (*vs.* 77% yield, Table 1, entry 6 *vs.* entry 5). This optimized protocol efficiently hydrogenates alkene **1a** using water as the main solvent and H_2SO_4 as the electrolyte, in contrast to conventional ECH methods that require more complex electrolytes (*e.g.*, nBu$_4$NPF$_6$) along with organic solvents (*e.g.*, MeCN, DMSO).[27,28]

Other organic solvents were also tested.[51,52] In ethylene glycol (Table 1, entry 7), a yield of 67% was obtained, whereas in acetone (Table 1, entry 8), the yield under the optimized [H_2SO_4]aq./solvent ratio (*i.e.* 3 : 1 v/v), was essentially the same as when using a [H_2SO_4]aq./solvent (1 : 1, v/v) (entry 8 *vs.* entry 1). A drop in the yield was observed when using a nickel foam of half the thickness (0.8 mm *vs.* 1.6 mm), to 47% yield, and when the electrode was compressed, to 31% yield (see ESI, Table S1, entries 13 and 14†). The use of galvanostatic conditions, in the range of −5 to −20 mA showed a low performance and poor selectivity (see ESI, Table S1, entries 18–21†).

Table 1 ECH of *p*-hydroxy benzylidene acetone (**1a**)

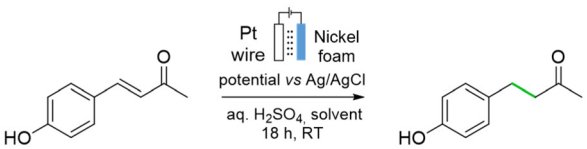

1a **2a**

Entry	Solvent	[H_2SO_4]aq. [M]	[H_2SO_4]aq. : solvent (v/v)	Potential [V]	Conv. (%)	Yield[a] (%)	FE (%)
1	Acetone	0.25	1 : 1	−2.5	99	56	3
2	MeOH	0.25	1 : 1	−2.5	87	73	<1
3	MeOH	0.25	1 : 1	−0.9	60	35	3
4	MeOH	0.38	3 : 1	−0.9	99	78	4
5	MeOH	0.19	3 : 1	−0.9	99	77	6
6	**EtOH**	**0.19**	**3 : 1**	**−0.9**	**99**	**89**	**10**
7	Ethylene glycol	0.19	3 : 1	−0.9	85	67	7
8	Acetone	0.19	3 : 1	−0.9	50	50	3

1a (0.4 mmol, 0.016 M). [a] Yield determined by ^{1}H NMR spectroscopy using an internal standard.

Table 2 ECH of 2-cyclohexanone (**1b**)

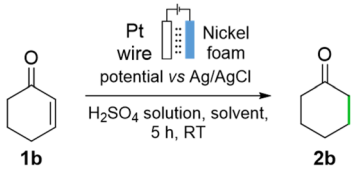

Entry	Solvent	$[H_2SO_4]$aq. [M]	$[H_2SO_4]$aq. : solvent (v/v)	Potential [V]	Conv. (%)	Yield[a] (%)	FE (%)
1	Acetone	0.25	1 : 1	−2.5	99	94	6
2	MeOH	0.25	1 : 1	−0.9	95	78	20
3	MeOH	0.38	3 : 1	−0.9	92	82	10
4	MeOH	0.19	3 : 1	−0.9	98	84	22
5	**EtOH**	**0.19**	**3 : 1**	**−0.9**	**97**	**90**	**24**
6[a,b]	EtOH	0.19	3 : 1	−0.9	87	79	9
7[a]	EtOH	0.19	3 : 1	−0.7	97	79	14
8[a,b]	EtOH	0.19	3 : 1	−0.7	58	52	26
9[a,b]	**EtOH**	**0.38**	**3 : 1**	**−0.7**	**96**	**94**	**37**

1b (0.4 mmol, 0.016 M). Yields were determined by GC-MS-FID using a calibration curve (see the ESI†). [a] 18 h. [b] 0.154 g scale (1.6 mmol).

Using an undivided cell was detrimental, giving a yield of 11% at a high conversion of 87% (Table S1, entry 27†), likely due to side reactions at the anode. Further details are presented in Table S1.†

We also optimized the ECH of 2-cyclohexenone (**1b**). Further, **1b** was chosen for the LCA due to its industrial relevance in the production of nylon 6 and other related materials.[53–55] In a mixture 1 : 1 (v/v) of acetone and H_2SO_4 (0.5 M aq.), a yield of 94% was obtained, however the FE was rather low (Table 2, entry 1). With the aim of improving the FE, MeOH was tested as the solvent at a milder potential of −0.9 V. This gave a significant improvement in the FE, and a small decrease in the yield of **2b** (Table 2, entry 2). We then varied the solvent ratio by increasing the amount of H_2SO_4 in the mixture (Table 2, entry 3), but this decreased the FE by a factor of 2. This lower FE is not surprising, due to the greater availability of protons for HER. When the reaction was run with the same ratio of aqueous/organic solvent (3 : 1, v/v), but with lower acidity (Table 2, entry 4), the FE and the yield both increased. When EtOH was used instead of MeOH under otherwise identical reaction conditions (Table 2, entry 5 *vs.* entry 4), both the yield and the FE (24%) increased further. The reaction was run on a larger scale (0.154 g, 1.6 mmol, entry 6), which gave a 79% yield and a FE of 9%. A lower potential could increase the FE, which occurred when the reaction was carried out at −0.7 V on a 0.4 mmol scale for 18 h (79% yield and FE of 14, Table 2, entry 7). An increase in concentration (0.064 M) led to a drop in conversion and yield (Table 2, entry 8). This was circumvented by an increase in acid concentration to 0.38 M, which resulted in an outstanding yield (94%) and significantly higher FE of 37%. Important to note is that there is a minimal production of organic byproducts (yield/conversion = 0.97), in addition to oxygen and dihydrogen gases which are discarded.

The catalyst recyclability was next assessed. Consecutive hydrogenation reactions of **1b** were run for reaction times of only 2 h, leading to yields of *ca.* 20%. This was so that we could compare activity differences (rates) from run to run, as well as differences in selectivities.[56] The nickel foam was washed with EtOH after every consecutive catalytic run. The performance showed little variation for 15 runs, giving **2b** in a 19.7 ± 1.6% yield (Fig. 2). After the completion of these 15 cycles, a decrease in mass of 7.24% was observed in the nickel foam. This is due to dissolution of Ni in the acidic media in the absence of electrical potential, which occurs during manipulation in between runs, as well as due to the sonication process required in the work-up. To rule out the leaching of nickel during operating conditions, a reaction was performed for 30 h as equivalent in time to the recyclability study (94% yield). No decrease in mass of the nickel foam electrode was detected after this test.

We then assessed the hydrogenation of **1b** using Pd/C and H_2 as the reductant. The reduction of **1b** using 1 mol% Pd/C gave, after 4 h, a yield of 52% of **2b** and 48% of phenol (Fig. 3, and Scheme S10†). The amount of phenol formed could be

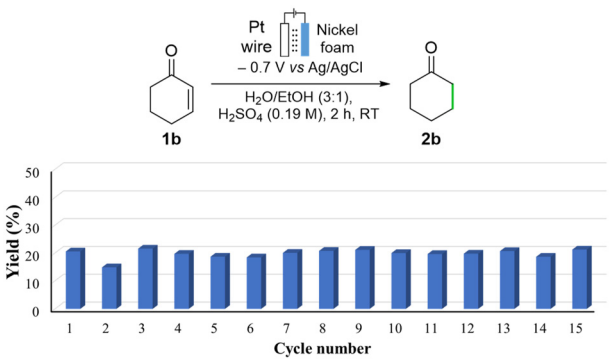

Fig. 2 Recyclability performance of the nickel foam at low conversion, after reaction times of 2 h. Yields were determined by GC-FID using a calibration curve.

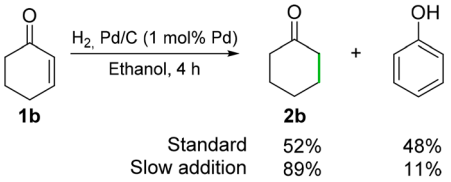

Fig. 3 Hydrogenation of 2-cyclohexenone (**1b**) with Pd/C and H_2.

decreased *via* slow addition of **1b** over 3.5 h. In contrast, phenol byproducts were never observed when the nickel foam system was used in the hydrogenation of **1b**. The recyclability of Pd/C was therefore assessed on alcohol **1a** instead, for which slow addition of the substrate was not needed. The system was tested over a series of 10 runs of 22 min each, and it showed a good but fluctuating performance, yielding **2a** in 29 ± 6.8% yields (Fig. 4). The reactions were carried out on a 1 g scale of **1a** (6.17 mmol), and the Pd/C catalyst was recovered by filtration (Scheme S10†). The mass loss of palladium was not tested due to its pyrophoric nature.

The outcomes of the life cycle impact assessment (LCIA) are summarized for both reaction systems in Fig. 5. The impact categories of the nickel foam system were all set to 100% for the internal normalization with the Pd/C system. The contributions for each impact category per functional unit are presented in the ESI (Section S4.2†). In general, the nickel foam method showed larger contributions for every impact category that we assessed. For human toxicity, ecotoxicity, eutrophication, and climate change, the nickel foam method represented an increase in the range of 1.5 to 6.3 times the contribution of the conventional Pd/C method.

For acidification and for resource use potential, a 14-fold and 50-fold increase was observed *vs.* the nickel foam method respectively. In both cases, the platinum counter electrode was the major contributor.

The identified hotspots that together contributed to at least 75% of the total impact in each category are shown in Fig. 5, and in Table S16 and Fig. S15.† For the nickel foam method, the platinum counter electrode production and electricity production were the main contributors. Similar results were observed for the Pd/C method, with electricity usage, and Pd catalyst production being the major hotspots. Interestingly, the preparation of nickel foam has a comparable impact to the preparation of the palladium catalyst, with contributions to acidification, human toxicity and ecotoxicity. The electricity consumption directly linked to the ECH represented only 0.26% of the total electricity consumption for a reaction performed at the laboratory scale, being the isolation of the products and the upstream processes responsible for the higher consumption of electricity. Furthermore, the impacts from Pd/C and nickel foam arise mainly from catalyst production, rather than from its use as a catalyst or its waste handling. Low impact from waste handling is however strongly related to the generic waste handling as modelled herein, as it does not quantitatively relate nickel or palladium potential long-term emissions from waste catalysts. The production of **2b**, used as model substrate for the screening LCA, became a concern for three impact categories for both scenarios. The size of the contribution can be expected to vary for different substrates. Hence, while potential impacts on resource use for the nickel foam catalyst is lower than that of the Pd/C catalyst, the screening LCA provided insights for further optimization of the environmental performance by addressing the use of the platinum counter electrode. Although ECH reactions are regarded as highly sustainable and environmentally benign,[57,58] the screening LCA conducted herein indicates that the environmental performance of the nickel foam hydrogenation method is hampered by the high potential impact of the platinum counter electrode. It should also be considered that the ECH of alkenes produces H_2 gas as by-product. Despite being valuable, this was treated as an emission to air due to the low scale of the reaction. In a scaled-up system, H_2 gas utilization would be feasible. This would give rise to an allocation issue where the environmental burden from the system would have to be shared between the two products, namely H_2 and alkane.[44] In practice, that could reduce the overall environmental impact of the isolated product in the nickel catalytic system.

The water-splitting process involves two simultaneous reactions: the HER and the Oxygen Evolution Reaction (OER). Protons, initially supplied from H_2SO_4, and then regenerated in the OER (*vide infra* and Section S4.1.1†), are consumed to form Ni–H species, leading to ECH of the substrate or to HER.[20] The OER requires a high potential, so it often becomes the limiting step in the overall electrochemical process.[24,59] Platinum and metal oxides such as RuO_2, IrO_2, and PtO_2 are highly active catalysts for the OER under acidic conditions, with variable levels of stability,[20,24,60] and more sustainable alternative options do not commercially exist. Consequently, the use of a platinum counter electrode remains the main limitation of the electrochemical method. However, the use of platinum as anode may be justified, bearing in mind its excellent stability under the mild reaction conditions used in this work (<1 V); under these conditions, Pt deactivation by irreversible formation of a platinum-oxide layer is avoided.[61] For

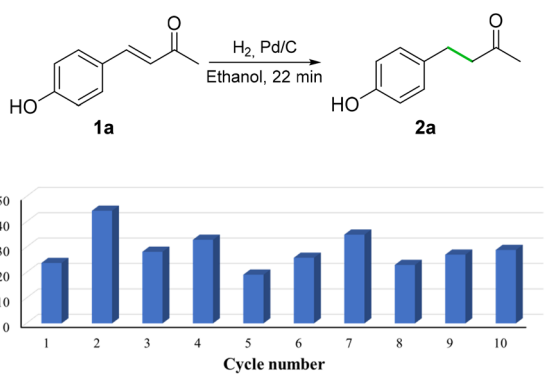

Fig. 4 Recyclability performance of the Pd/C and H_2 method at low conversions, after reaction times of 22 min. Yields were determined by ^{1}H NMR spectroscopy using an internal standard.

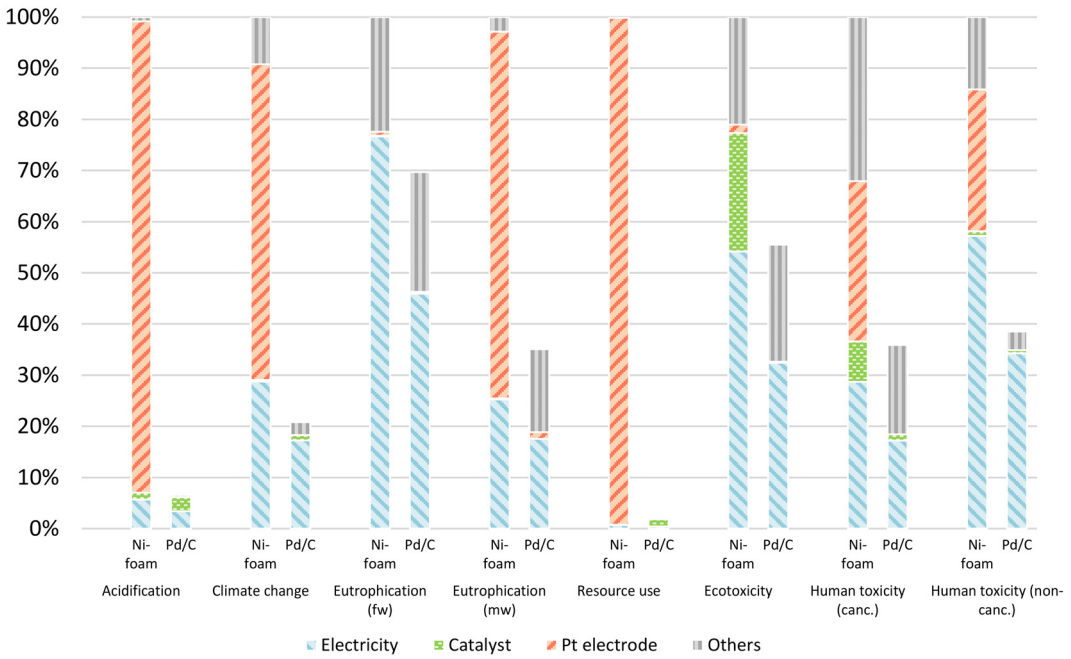

Fig. 5 Normalized contribution for the different impact categories based on the indicative screening LCA. Catalyst stands for Pd and nickel foam for the Pd/C and nickel foam systems, respectively.

the LCIA, we considered reusing the platinum electrode for 1500 cycles and estimated that it would take 600 000 cycles of reuse for its contribution to total impacts in the resource use impact category to drop below 25%. While this may be feasible, the scarcity of platinum is a significant reason to consider replacing this electrode. Graphite has been extensively used as anode for applications in batteries and electrochemical reactions with excellent performance.[62–66] Graphite could potentially be a promising alternative due to its higher abundance and stability, although the latter might be compromised in acidic conditions.[60,62–68] Regarding the environmental impact of graphite, several assessments indicate a possible lower global warming potential in comparison with platinum (see Section S4.1.3.†). However, the high energy consumption required in graphite production, together with the limited available data for its evaluation increase the uncertainty about graphite depicting a lower environmental impact.[62,66]

The replacement of platinum electrodes by carbon-based electrodes was studied for its use in the electrochemical reaction. Several carbon-based counter electrodes were tested (Table 3). Carbon paper and carbon cloth were used as anodes, and moderate yields were obtained in the hydrogenation of **1a** (Table 3, entries 2 and 3). An increase in surface area did not result in any improvement of performance (Table 3, entry 4). When using a graphite rod as counter electrode, a promising 77% yield was obtained with EtOH as cosolvent (Table 3, entry 5). When EtOH was replaced by *n*BuOH as cosolvent (*vide infra*), product **2a** was obtained in 97% yield (Table 3, entry 6). The recyclability properties of graphite as anode were evaluated (Scheme S1†). A larger surface area was employed to ensure exposure to the acidic solution (23 *vs.* 16 cm^2). Upon

Table 3 Pt *vs.* C-based counter electrodes

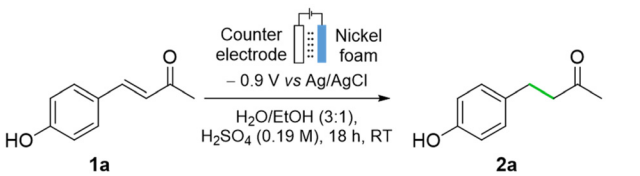

Entry	Counter electrode	Surface[a] [cm^2]	Yield[b] [%]
1	**Pt wire**	**13**	**89**
2	Carbon paper	16	45
3	Carbon cloth	16	40
4	Carbon cloth	40	48
5	Graphite	16	77
6[c]	**Graphite**	**16**	**97**

1a (0.4 mmol, 0.016 M). [a] Geometric surface. [b] Yields were determined by ^{1}H NMR spectroscopy using an internal standard. [c] Using aqueous H_2SO_4 (0.25 M) and *n*BuOH as cosolvent (7% v/v).

hydrogenation of **1b** in short reaction times (2 h), **2b** was obtained in 41 ± 4.8% yield for each of the 15 runs (see ESI, Scheme S1†), with a small mass decrease of 1.4% of the graphite mass after run 15, indicating that the graphite rod may potentially be a good alternative to platinum-based anodes.

As electricity production was a relevant hotspot for both baseline scenarios (nickel foam and Pd/C catalytic systems), we carried out a future scenario assessment for both methods, in which the Swedish electricity production grid mix was changed to a proposed reasonable future electricity grid mix for the year 2030 (Fig. 6).[43] The modelled future scenario

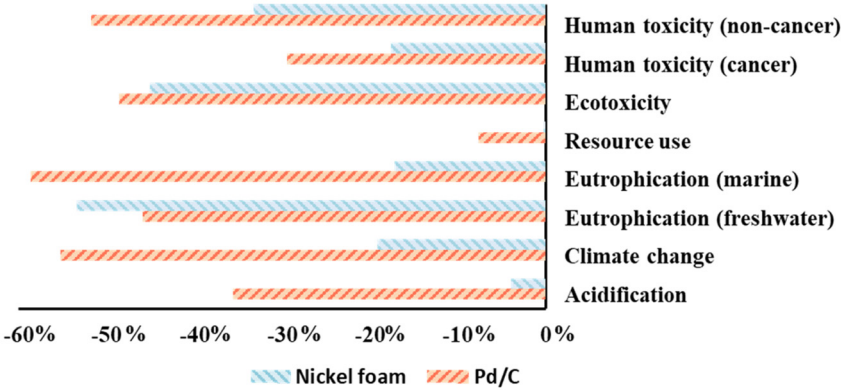

Fig. 6 Impact reduction per each impact category for the theoretical future scenario using a proposed 2030 energy mix.

showed a decrease in the overall environmental impact for both methods (see ESI, Section S4.2.2†). This results from an estimated higher share of renewable electricity, especially wind energy (see also ESI, Table S17†).

A significant improvement was observed for those impact categories that are highly dependent on electricity production at any point in the cradle-to-gate timeframe, irrespective of whether the method is electrochemical or not. For the nickel foam method, a decrease in impact was found for all impact categories, with an improvement of up to 53% found for eutrophication (Fig. 6). The Pd/C method showed a similar trend, with improvements of up to 59% for the same impact category (see ESI, Section S4.2.2†).

We continued catalysts evaluation by assessing potential safety and toxicological hazards based on the available data provided by manufacturers and importers under REACH and CLP notifications, as well as whether the substance is defined under harmonised classification and labelling (CLH) (see Scheme S5†).[47] From a physical safety perspective, the pyrophoric nature of Pd/C combined with the flammability of H_2 represents a major safety concern. This is circumvented in the nickel foam method, as there is no source for ignition, the amounts of H_2 produced during operation are low, and the anode materials (graphite and platinum) show no hazards. The use of water as source of hydrogen atoms avoids the transportation and storage of H_2, improving the safety of the overall process. Regarding toxicity, while the nickel foam method raises significant concerns related to skin sensitization (H317) properties and potential organ damage upon prolonged or repeated exposure (H372), it remains a minor issue in a safe laboratory environment where exposure can be kept to a minimum.

Under the acidic reaction conditions, $NiCl_2$ or $NiSO_4$ salts may be formed (see ESI, Section S3.4 and Scheme S5†). $NiCl_2$ is formed when an aqueous HCl solution is used in the nickel foam activation step. The replacement of this acid by H_2SO_4 enabled us to avoid formation of Cl_2 and $NiCl_2$. As a result, $NiSO_4$ is formed instead, which poses a lower risk than $NiCl_2$. The degree of loss of Ni from the system is very low, as demonstrated under continuous operation. Neither platinum nor graphite electrodes pose any safety concerns. Palladium is generally classified without any major hazards according to ECHA classifications.[47] However, it's important to acknowledge that palladium is produced or imported in smaller quantities in Europe compared to nickel, and the registration requirements for palladium are less stringent. The main risks associated with palladium arise from its pyrophoricity, and certain manipulation precautions are necessary to avoid accidents and exposure.

To complement the toxicological assessment for the nickel foam system, we identified the byproducts formed in the ECH of **1b** (Fig. 7). Formation of cyclohexanol **3b**, 1,1-diethoxycyclohexane **4**, and 3-ethoxycyclohexanone **5** as byproducts was observed, however in less than 0.5%, 0.5%, and 1.8% yield, respectively. Their concentrations were determined by GC-FID using a calibration curve (see the ESI, Scheme S14†). None of these compounds represents a toxicological hotspot in comparison with other components in the reaction mixture.

Recognizing the greater abundance of nickel compared to palladium, the nickel foam system holds promise as a potential alternative to the conventional Pd system, and thus we proceeded to explore the scope and limitations of the method when applied to a variety of mono-, di-, and trisubstituted alkenes (Fig. 8 and 9). Pt counter electrode and EtOH were used for the scope due to their robustness and availability, respectively. Unfunctionalized and electron-rich substituted benzylidene acetones gave the corresponding products **2c–2f** in yields ranging from 55 to 77%. Alkene **1g**, with a bromide substituent on the aryl group, gave reduced **2g** in 42% yield.

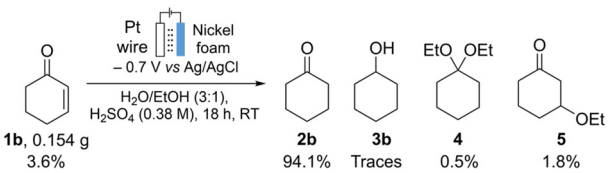

Fig. 7 Identification and quantification of the byproducts in the electrochemical hydrogenation of **1b**.

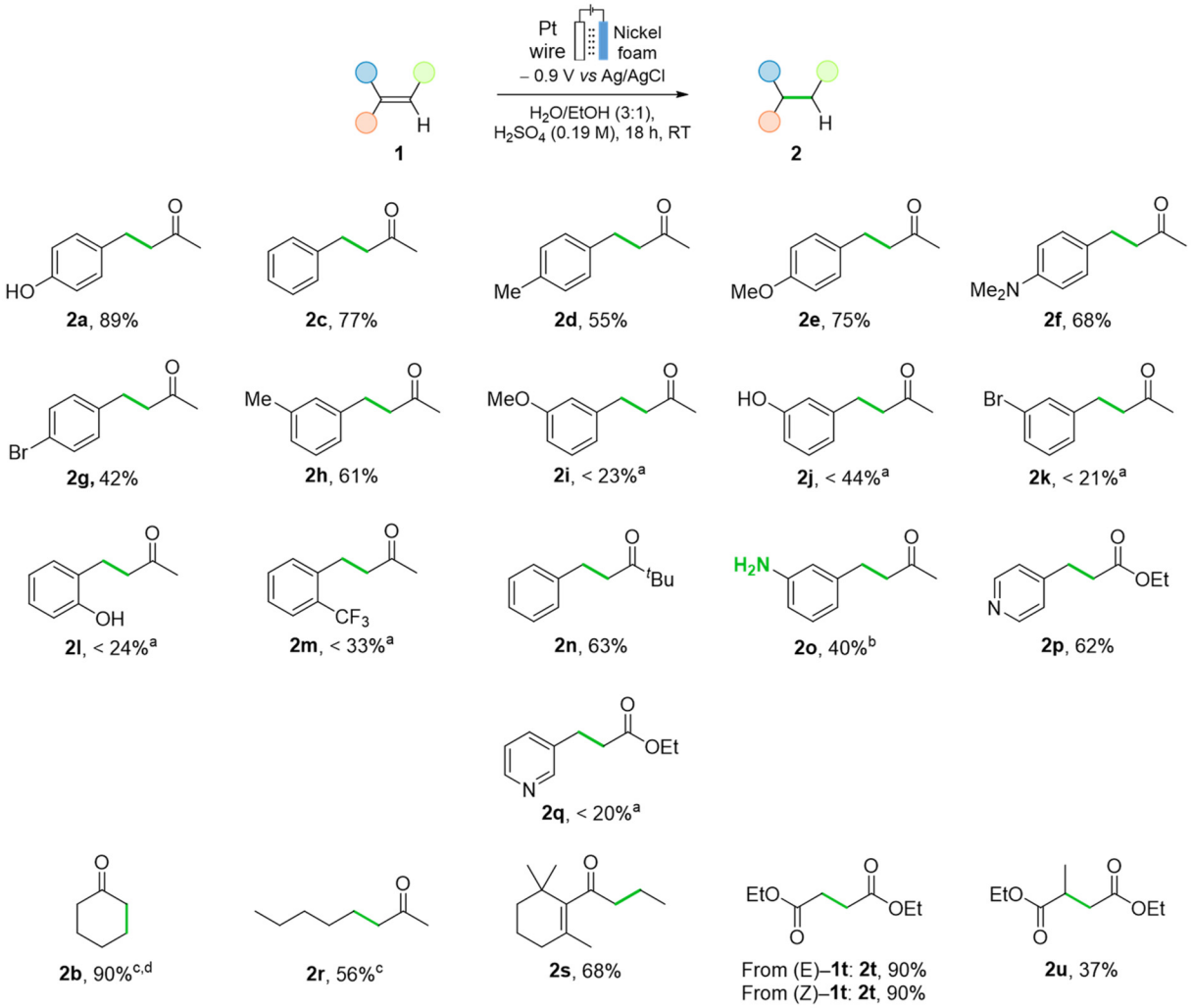

Fig. 8 Substrate scope and limitations. **1** (0.4 mmol, 0.016 M). [a]Yields were determined by ^{1}H NMR spectroscopy using an internal standard. [b]H_2SO_4 concentration was 0.38 M. [c]Yields were determined by GC-FID using a calibration curve. [d]5 h.

m-Substituted benzylidene acetones **1h–1k** showed a diverse reactivity.

The *m*-methyl-substituted derivative gave the desired product **2h** in a good 61% yield, but a significant drop in performance was observed for the corresponding methoxy, hydroxy, and bromo derivatives. Products **2i–2k** and were obtained in 23%, 44%, and 21% yields, respectively. The influence of steric hindrance was confirmed by the poor performance of *o*-substituted benzylidene acetones **1l** and **1m** (24 and 33% NMR yields, respectively). Hindrance on the α-carbon of the enone was relatively well tolerated, as shown in the hydrogenation of *tert*-butyl ketone **1n** (63% yield). Interestingly, the hydrogenation of both the alkene and the nitro groups in **1o** took place when the acidity was increased slightly, yielding **2o** was obtained in 40% yield. The presence of a substituted pyridine and an ester group were tolerated, and the corresponding saturated derivative **2p** was obtained in 62% yield. *m*-Pyridinyl analogue **1q** reacted in a significantly lower 20% NMR yield. Iodo, thiophene and amide moieties were not tolerated, often depicting no conversion (see ESI, Section S2.6†).

Regarding non-aromatic enones, 2-cyclohexenone **1b** was hydrogenated to give **2b** in 90% yield within 5 h. Aliphatic 3-octen-2-one underwent hydrogenation into **2r** in 56% yield. β-Damascone, contributor to the smell of roses, was hydrogenated to **2s** in a high of 68% yield. We assessed whether the *E*/*Z* configuration of the double bond had an influence on the reaction outcome: both diethyl fumarate and diethyl maleate underwent the hydrogenation to give diethyl succinate **2t** in 90% yield in both cases. The hydrogenation of trisubstituted alkenes proved to be more challenging; diethyl mesaconate was hydrogenated to give **2u** in 37% yield. Excellent selectivity for alkene *vs.* ketone hydrogenation was observed in all cases, being the resulting alcohols detected only in trace amounts. This chemoselectivity represents an advantage of the Ni-system over the Pd/C one, as the latter produces *ca.* 20% yield of the fully hydrogenated alcohols during the hydrogenations of **1a**, **1f**, **1g** and **1o** (Schemes S12

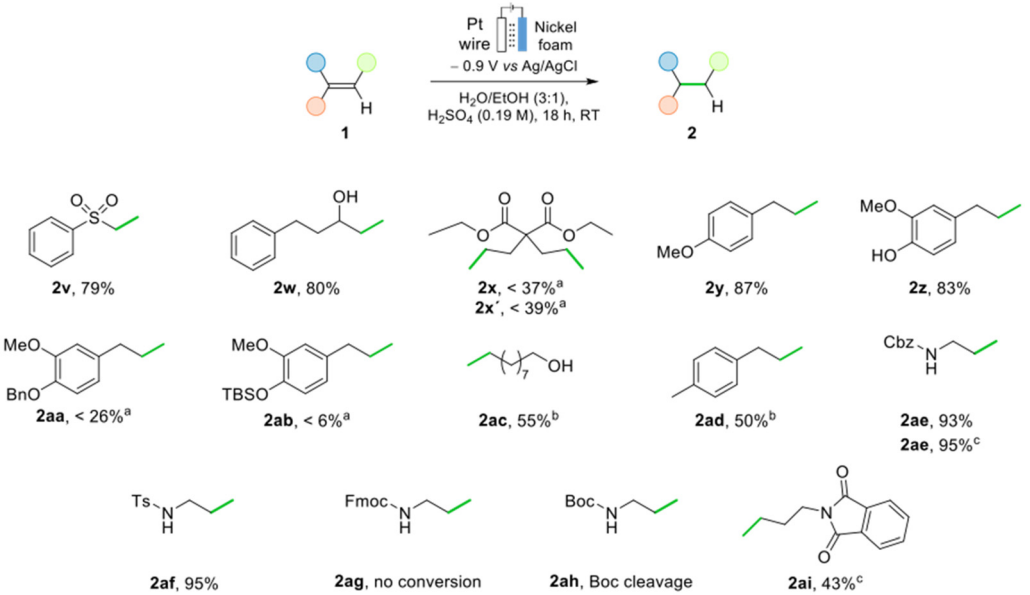

Fig. 9 Substrate scope and limitations. **1** (0.4 mmol, 0.016 M). [a]Yields were determined by ^{1}H NMR spectroscopy using an internal standard. [b]Yields were determined by GC-FID using a calibration curve. [c]From alkyne.

and S13†). No dimerization products from radical homocoupling were observed.

Other types of alkene substitutions were explored apart from enones (Fig. 9). Vinyl sulfone **1v** and allyl alcohol **1w** were hydrogenated in high 79% and 80% yield, respectively. When applying the method to conjugated alkenes, no conversion was observed (ESI, Section 2.6†). However, if the alkenes are not conjugated, as in **1x** and **1x′** yields of 37% and 39% were obtained, respectively. The terminal alkenes estragole and eugenol gave **2y** and **2z** in high yields of 87% and 83%, respectively. To demonstrate the mild conditions of the protocol, we explored the tolerance to different protecting groups. Benzyl- and TBS-protected alcohols, despite being tolerated under the reaction conditions, afforded very low conversions into **2aa** and **2ab**. No products from hydrogenolysis or deprotection were observed. The conversion could be improved significantly when replacing EtOH by *n*BuOH, to 75% and 60% yield, respectively (*vide infra*). 9-Decen-1-ol **1ac** and allyl toluene **1ad** were hydrogenated to the corresponding products **2ac** and **2ad** in moderate yields.

Amino protecting groups *N*-Cbz and *N*-tosyl were tolerated (93% and 95% yield of **2ae** and **2af**, respectively). Although tolerated, *N*-Fmoc protected amine (**1ag**) gave no conversion, and Boc-allyl amine **1ah** decomposed under the reaction conditions. The ECH of allyl alcohol **1ao** and of allyl amine **1an** gave the corresponding products in low yields. A low mass balance was observed due to their volatility and good solubility in aqueous media (see ESI, Section 2.6†). The same method was used for the direct hydrogenation of alkynes into saturated derivatives; *N*-Cbz protected propargyl amine **1aj** and *N*-(3-butynyl)phthalimide (**1ai**) gave fully saturated **2ae** and **2ai** in 95% and 43% yield respectively. For substrates that suffered from low solubility, a solvent screening was performed (see ESI, Table S5†). The use of *n*BuOH, one of the greenest solvents,[49,52,69] showed an increase in yield from 26% yield in EtOHto 75% in *n*BuOH for benzyl eugenol **1aa**. With these conditions, some substrates were re-examined (Fig. 10). Bromo benzylidene acetone **1g** yield increased from 42% to 59% yield, with simultaneous reduction in the formation of side products. For *m*-substituted enones **1i** and **1j**, this change led to yields of 72% and 82%, from 23% and 44% yield, respectively. Furthermore, the hydrogenation of TBS protected eugenol to **2ab** was achieved in 60% yield upon an increase in acid concentration. Achieving high faradaic efficiencies (FEs) for ECH in aqueous acidic conditions is difficult due to the relatively low potential at which the hydrogen evolution reaction (HER) occurs.[18]

A series of control experiments were performed. The process is electromediated, since it requires continuous potential to observe hydrogenation, which does not occur when pure hydrogen gas (H_2) is used without applied potential (see ESI, Table S1, entries 23 and 24†). This indicates that the Ni–H_{ads} species, formed directly upon potential application, are the species responsible for the hydrogenation, and that H_2 production is a side reaction.[18,70] The use of 1,1-diphenylethylene and *tert*-butanol as additives[30] had a detrimental effect on the reaction. These additives react with Ni–H* forming stable ethane-1,1-diyldibenzenyl and *tert*-butyl radicals respectively (see ESI, Table S1, entries 28 and 29†). Thus, Ni–H_{ads} species are the key intermediates in the ECH of alkenes. Analysis *via* cyclic voltammetry of **1a** did not show any direct electron transfer nor current when having EtOH as the only solvent, ruling out a possible electro-mediated hydrogen transfer mechanism (see ESI, Fig. S4†). The absence of an additional process in the range of the ECH ($V \geq 0.7$ V) rules out the Proton-Coupled

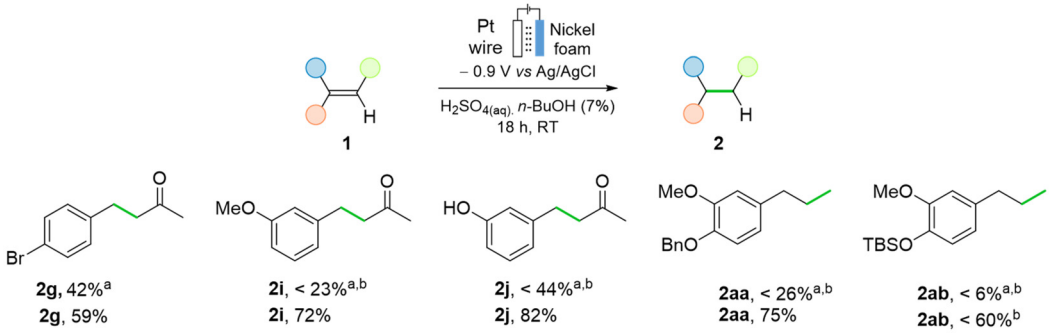

Fig. 10 Substrate scope and limitations using *n*BuOH as cosolvent instead of EtOH. 1 (0.4 mmol, 0.016 M). [a]Using aqueous H_2SO_4 (0.19 M)/EtOH (3 : 1). [b]Yields were determined by ^1H NMR spectroscopy using an internal standard.

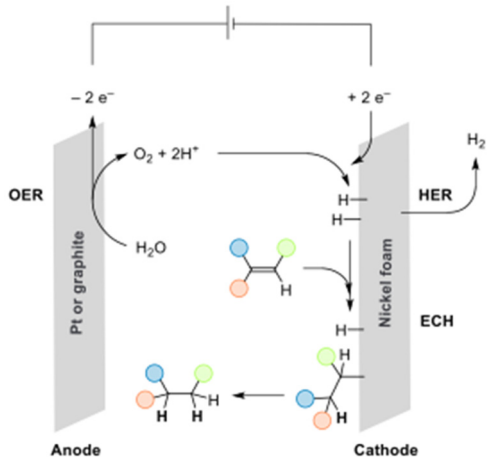

Fig. 11 Proposed mechanism for the ECH of alkenes using nickel foam in acidic aqueous media.

Electron Transfer (PCET) for the ECH. The proposed mechanism is shown in Fig. 11, in which protons generated from OER migrate to the cathode. Protons undergo the Volmer step leading to neutral adsorbed hydrogen, followed by the ECH of alkenes *via* addition of H_{ads}.

A kinetic profile of the reduction of *N*-Cbz-protected propargylic amine (**1aj**) is presented in Fig. S5,† which shows that comparable amounts of Cbz-protected allyl amine (**1ae**) and Cbz-protected propyl amine (**2ae**) are formed at short reaction times. This indicates that the reduction rates of alkyne and alkene are within the same order of magnitude under the conditions used.

Conclusions

The catalytic hydrogenation of alkenes using an unfunctionalized nickel foam was developed and further optimized for environmental performance and safety by using screening life cycle assessment as well as safety and toxicological assessments. The method can achieve moderate to high yields from a variety of tri-, di- and monosubstituted enones and alkenes with excellent selectivity *vs.* C=O reduction with FE up to 37% despite the use of an aqueous acidic solution as main solvent. Homocoupling products were also avoided. The system requires an organic cosolvent, and two solvents, with minimum hazard profile, EtOH or *n*BuOH, were successfully identified to enable the catalytic reaction. This method can be seen as an alternative to the use of electrolytes such as nBu_4NPF_6 and solvents such as MeCN and DMSO, which are frequently used in ECH. The use of *n*BuOH as the solvent was particularly important when substrates with low solubility were used. The recyclability properties of the nickel foam were assessed, showing a constant performance for at least 15 runs. The physical and toxicological hazard assessment informed about a trade-off between physical safety and toxicity when comparing the use of the Ni-mediated electrochemical method reported here with that of the conventional Pd/C and H_2 gas. Interestingly, despite the abundance of nickel *vs.* palladium being a driving force for using the electrochemical method, the screening LCA results indicate that the Pt counter electrode would need to be reused more than 600 000 cycles, to arrive at an estimated lower impact in the resource use category compared to the Pd/C reaction system. Alternatively, the Pt counter electrode may be exchanged by a graphite rod, which, despite a lower stability under the reaction conditions, could present a lower environmental impact. In addition, the screening LCA identified additional hotspots, mainly related to energy use, that should be considered in future applications of the nickel foam method to improve its environmental performance further.

Despite the lower impact depicted for the Pd system *vs.* the nickel foam method when using Pt as counter electrode, palladium consumption must be minimized in the near future due to its the scarcity. A transition to more abundant metals becomes soon mandatory. The understanding of the new method's sustainability is an important tool to develop them further, so that they do not compromise the well-being of our future generations.

Abbreviations

ECH	Electrochemical hydrogenation
FE	Faradaic efficiency

HER Hydrogen evolution reaction
LCA Life cycle assessment
LCI Life cycle inventory
LCIA Life cycle impact assessment
OER Oxygen evolution reaction.

Author contributions

PJT, PMP and BMM conceptualized the project. PJT and PMP performed the hydrogenations and the data analysis. TK, PJT and HH collected the data and treated the data for LCA. CN contributed with data for toxicological assessments together with PJT. All authors contributed to the analysis of results. The manuscript was written through contributions from all authors. All authors have given approval to the final version of the manuscript.

Data availability

This article has been previously preprinted.[71]

The data supporting this article have been included as part of the ESI.† All original code will be deposited at Zenodo and it will be publicly available as of the date of publication at **https://doi.org/zenodo.14204532**.

The data supporting the submitted work can be found in the ESI of the article. The ESI also contains further details regarding safety, toxicological and life cycle assessments, as well as characterization information of the prepared compounds (^{1}H NMR, ^{13}C NMR, ^{19}F NMR, GC-FID-MS, and HRMS).†

The raw NMR data files for all compounds reported in the article are deposited at Zenodo and will be made *publicly available after acceptance*. The numbering of the files will then be matched to those in the article. Each parent folder in Zenodo will contain subfolders with different files. In order to process the data, the full parent folder must be dragged into either Mestrenova or Topspin and then the data is automatically processed. If the name of the raw data files are renamed, the software (Mestrenova or Topspin) will not be able to process the files.

Conflicts of interest

There are no conflicts to declare.

Acknowledgements

The authors gratefully acknowledge the Swedish Foundation for Strategic Environmental Research (Mistra SafeChem, project number 2018/11) and the Swedish Research Council through Vetenskapsrådet. Knut and Alice Wallenberg Foundation (KAW 2016.0072) and the Göran Gustafsson Foundation are also gratefully acknowledged. We thank AstraZeneca and Stockholm University for generous support. We also thank Ian Cotgreave and Georgios Giovanoulis for helpful discussions, and Alejandro Valiente for preliminary investigations. All authors thank Astra-Zeneca and Stockholm University for support.

References

1 F. Zaera, The surface chemistry of Metal-based hydrogenation catalysis, *ACS Catal.*, 2017, **7**, 4947–4967.
2 M. A. Stoffels, F. J. R. Klauck, T. Hamadi, F. Glorius and J. Leker, Technology trends of catalysts in hydrogenation reactions: a patent landscape analysis, *Adv. Synth. Catal.*, 2020, **362**, 1258–1274.
3 A. Narani, K. H. P. Reddy, K. Natte and D. R. Burri, Pd-Nanoparticles immobilized organo-functionalized SBA-15: an efficient heterogneous catalyst for selective hydrogenation of C–C double bonds of α,β-unsaturated carbonyl compounds, *Mol. Catal.*, 2020, **497**, 111200.
4 P. Nuss and M. J. Eckelman, Life cycle assessment of metals: a scientific synthesis, *PLoS One*, 2014, **9**, e101298.
5 L. Lloyd, Hydrogenation Catalysts, in *Handbook of Industrial Catalysts*, Springer US, Boston, 2011, pp. 73–117.
6 H. Chen and J. Sun, Selective hydrogenation of phenol for cyclohexanone: a review, *J. Ind. Eng. Chem.*, 2021, **94**, 78–91.
7 S. Kar, H. Sanderson, K. Roy, E. Benfenati and J. Leszczynski, Green chemistry in the synthesis of pharmaceuticals, *Chem. Rev.*, 2022, **122**, 3637–3710.
8 T. Chandra and J. P. Zebrowski, Hazards associated with laboratory scale hydrogenations, *J. Chem. Health Saf.*, 2016, **23**, 16–25.
9 R. M. Navarro, M. A. Peña and J. L. G. Fierro, Hydrogen production reactions from carbon feedstocks: fossil fuels and biomass, *Chem. Rev.*, 2007, **107**, 3952–3991.
10 P. J. Megía, A. J. Vizcaíno, J. A. Calles and A. Carrero, Hydrogen production technologies: from fossil fuels towards renewable sources. A mini review, *Energy Fuels*, 2021, **35**, 16403–16415.
11 A. G. Campaña, R. E. Estévez, N. Fuentes, R. Robles, J. M. Cuerva, E. Buñuel, D. Cárdenas and J. E. Oltra, Unprecedented Hydrogen Transfer from Water to Alkenes and Alkynes Mediated by Ti^{III} and Late Transition Metals, *Org. Lett.*, 2007, **9**, 2195–2198.
12 J. Rosales, T. Jiménez, R. Chahboun, M. A. Huertos, A. Millán and J. Justicia, Mild and Selective Hydrogenation of Unsaturated Compounds Using Mn/Water as a Hydrogen Gas Source, *Org. Lett.*, 2024, **26**, 2147–2151.
13 T. Sato, S. Watanabe, H. Kiuchi, S. Oi and Y. Inoue, Hydrogenation of Olefins Using Water and Zinc Metal Catalyzed by a Rhodium Complex, *Tetrahedron Lett.*, 2006, **47**, 7703–7705.
14 E. Zhao, W. Zhang, L. Dong, R. Zbořil and Z. Chen, Photocatalytic Transfer Hydrogenation Reactions Using Water as the Proton Source, *ACS Catal.*, 2023, **13**, 7557–7567.

15 C. H. Lam, C. B. Lowe, Z. Li, K. N. Longe, J. Y. Rayburn, M. A. Caldwell, C. E. Houdek, J. B. Maguire, C. M. Saffron, D. J. Miller and J. E. Jackson, Electrocatalytic upgrading of model lignin monomers with earth abundant metal electrodes, *Green Chem.*, 2015, **17**, 601–609.
16 T. Ali, H. Wang, W. Iqbal, T. Bashir, R. Shah and Y. Hu, Carbon-Based Electrocatalysts for Hydrogen and Oxygen Evolution Reactions, *Adv. Sci.*, 2023, **10**, 2205077.
17 Z. Shi, N. Li, H.-K. Lu, X. Chen, H. Zheng, Y. Yuan and K.-Y. Ye, Recent advances in the electrochemical hydrogenation of unsaturated hydrocarbons, *Curr. Opin. Electrochem.*, 2021, **28**, 100713.
18 J. A. Lopez-Ruiz, E. Andrews, S. A. Akhade, M.-S. Lee, K. Koh, U. Sanyal, S. F. Yuk, A. J. Karkamkar, M. A. Derewinski, J. Holladay, V.-A. Glezakou, R. Rousseau, O. Y. Gutiérrez and J. D. Holladay, Understanding the role of metal and molecular structure on the electrocatalytic hydrogenation of oxygenated compounds, *ACS Catal.*, 2019, **9**, 9964–9972.
19 C. Li and J.-B. Baek, Recent advances in noble metal (Pt, Ru, and Ir)-based electrocatalysts for efficient hydrogen evolution reaction, *ACS Omega*, 2020, **5**, 31–40.
20 Y. Yan, B. Y. Xia, B. Zhao and X. Wang, A review on noble-metal-free bifunctional heterogeneous catalysts for overall electrochemical water splitting, *J. Mater. Chem. A*, 2016, **4**, 17587–17603.
21 P. C. K. Vesborg and T. F. Jaramillo, Adressing the terawatt challenge: scalability in the supply of chemical elements for renewable energy, *RSC Adv.*, 2012, **2**, 7933–7947.
22 J. R. Ludwig and C. S. Schindler, Catalyst: sustainable catalysis, *Chem*, 2017, **2**, 313–316.
23 *CRC Handbook of Chemistry and Physics*, ed. W. M. Haynes, CRC press, Boca Raton, 97th edn, 2016, pp. 14–17.
24 N. K. Chaudhari, H. Jin, B. Kim and K. Lee, Nanostructured materials on 3D nickel foam as electrocatalysts for water splitting, *Nanoscale*, 2017, **9**, 12231–12247.
25 X. Yang, W. Li, T. Ai, W. Bao, H. Dong, P. Jiang and X. Zou, An efficient hydrogen evolution by self-supported nickel sulfur-based hybrid nanoplate electrocatalyst, *Ionics*, 2022, **28**, 353–360.
26 W. Liu, Y. Peng, H. He, W. Tan, Y. Chen and X. Dai, A novel Ni-La-Nd-Y flim on Ni foam to enhance hydrogen evolution reaction in alkaline media, *Int. J. Hydrogen Energy*, 2022, **47**, 10289–10297.
27 For a review, see:J. Yang, H. Qin, K. Yan, X. Cheng and J. Wen, Advances in electrochemical hydrogenation since 2010, *Adv. Synth. Catal.*, 2021, **363**, 5407–5416and references therein.
28 Y. Zhang, X. Zhao and G. Qing, Electrochemical-induced hydrofunctionalizations of alkenes and alkynes, *Chem. Synth.*, 2024, **4**, 16, and references therein.
29 Y. Ling, Y. Wu, C. Wang, C. Liu, S. Lu and B. Zhang, Selenium vacancy promotes transfer semihydrogenation of alkynes from water electrolysis, *ACS Catal.*, 2021, **11**, 9471–9478.
30 A. Valiente, P. Martínez-Pardo, G. Kaur, M. J. Johansson and B. Martín-Matute, Electrochemical proton reduction over a nickel foam for Z-stereoselective semihydrogenation/deuteration of functionalized alkynes, *ChemSusChem*, 2022, **15**, e202102221.
31 L. Behrouzi, Z. Zand, M. Fotuhi, B. Kaboudin and M. M. Najafpour, Water oxidation couples to electrocatalytic hydrogenation of carbonyl compounds and unsaturated carbon-carbon bonds by nickel, *Sci. Rep.*, 2022, **12**, 19968.
32 P. Anastas and N. Eghbali, Green chemistry: principles and practice, *Chem. Synth.*, 2010, **39**, 301–312.
33 C. Caldeira, R. Farcal, I. Garmendia Aguirre, L. Mancini, D. Tosches, A. Amelio, K. Rasmussen, H. Rauscher, J. Riego Sintes and S. Sala, *Safe and sustainable by design chemicals and materials: framework for the definition of criteria and evaluation procedure for chemicals and materials*. Publications Office of the European Union, 2022.
34 G. S. Bhander, M. Hauschild and T. McAloone, Implementing life cycle assessment in product development, *Environ. Prog.*, 2003, **22**, 255–267.
35 M. L. Parisi, A. Dessì, L. Zani, S. Maranghi, S. Mohammadpourasi, M. Calamante, A. Mordini, R. Basosi, G. Reginato and A. Sinicropi, Combined LCA and green metrics approach for the sustainability assessment of an organic dye synthesis on lab scale, *Front. Chem.*, 2020, **8**, 214.
36 A. Santos, P. Yustos, A. Quintanilla, F. García-Ochoa, J. A. Casas and J. J. Rodríguez, Evolution of toxicity upon wet catalytic oxidation of phenol, *Environ. Sci. Technol.*, 2004, **38**, 133–138.
37 Swedish Chemicals Agency. **https://www.kemi.se/en/publications/guidance-on-national-chemicals-control-for-other-countries/hazard-and-risk-assessment-of-chemicals—an-introduction**. (Accessed February 2023).
38 F. Grimaldi, G. A. de Leon Izeppi, D. Kirschneck, P. Lettieri, M. Escribà-Gelonch and V. Hessel, Life cycle assessment and cost evaluation of emerging technologies at early stages: the case of continuous flow synthesis of Rufinamide, *J. Adv. Manuf. Process.*, 2020, **2**(2), e10043.
39 N. Thonemann, A. Schulte and D. Maga, How to conduct life cycle assessment for emerging technologies? A systematic review and methodological guidance, *Sustainability*, 2020, **12**, 1192.
40 X. Liu and D. Astruc, Development of the applications of palladium on charcoal in organic synthesis, *Adv. Synth. Catal.*, 2018, **360**, 3426–3459.
41 B. Chen, U. Dingerdissen, J. G. E. Krauter, H. G. J. Lansink Rotgerink, K. Möbus, D. J. Ostgard, P. Panster, T. H. Riermeier, S. Seebald, T. Tacke and H. Trauthwein, New developments in hydrogenation catalysis particularly in synthesis of fine and intermediate chemicals, *Appl. Catal., A*, 2005, **280**, 17–46.
42 G. Finnveden, M. Z. Hauschild, T. Ekvall, J. Guinee, R. Heijungs, S. Hellweg, A. Koehler, D. Pennington and S. Suh, Recent developments in life cycle assessment, *J. Environ. Manage.*, 2009, **91**, 1–21.

43 IEA Energy Statistics Data Browser. https://www.iea.org/data-and-statistics/data-tools/energy-statistics-data-browser (accessed August 2022).
44 R. K. Rosenbaum, T. M. Bachmann, L. S. Gold, M. A. J. Huijbregts, O. Jolliet, R. Juraske, A. Koehler, H. F. Larsen, M. MacLeod, M. Margni, T. E. McKone, J. Payet, M. Schuhmacher, D. van de Meent and M. Z. Hauschild, USEtox – the UNEP-SETAC toxicity model: recommended characterisation factors for human toxicity and freshwater ecotoxicity in life cycle impact assessment, *Int. J. Life Cycle Assess.*, 2008, **13**, 532–546.
45 M. Z. Hauschild, M. Huijbregts, O. Julliet, M. MacLeod, M. Margni, D. van de Meent, R. K. Rosenbaum and T. E. McKone, Building a model based on scientific consensus for life cycle impact assessment of chemicals: the search for harmony and parsimony, *Environ. Sci. Technol.*, 2008, **42**, 7032–7037.
46 European Platform on LCA. https://eplca.jrc.ec.europa.eu/LCDN/developerEF.xhtml. (Accessed September 2022).
47 European Chemicals Agency. https://echa.europa.eu/regulations/clp/harmonised-classification-and-labelling (Accessed February 2023).
48 D. G. Barceloux, G. Randall Bond, E. P. Krenzelok, H. Cooper and J. A. Vale, American academy of clinical toxicology practice guidelines on the treatment of methanol poisoning, *J. Toxicol., Clin. Toxicol.*, 2002, **40**, 415–446.
49 D. Prat, A. Wells, J. Hayler, H. Sneddon, C. R. McElroy, S. Abou-Shehada and P. J. Dunn, CHEM21 selection guide of classical- and less classical- solvents, *Green Chem.*, 2016, **18**, 288–296.
50 J. van den Broek, S. Abegg, S. E. Pratsinis and A. T. Güntner, Highly selective detection of methanol over ethanol by a handheld gas sensor, *Nat. Commun.*, 2019, **10**, 4220.
51 Y.-Q. Jiang, J. Li, Z.-W. Feng, G.-Q. Xu, X. Shi, Q.-J. Ding, W. Li, C.-H. Ma and B. Yu, Ethylene glycol: a green solvent for visible light-promoted aerobic transition metal-free cascade sulfonation/cyclization reaction, *Adv. Synth. Catal.*, 2020, **362**, 2609–2614.
52 M. Tobiszewski, J. Namieśnik and F. Pena-Pereira, Environmantal risk-based ranking of solvents using the combination of a multimedia model and muti-criteria decision analysis, *Green Chem.*, 2017, **19**, 1034–1042.
53 K. F. Podraza, Regiospecific alkylation of cyclohexenones: a review, *Org. Prep. Proced. Int.*, 1991, **23**, 217–235.
54 T. Diao and S. S. Stahl, Synthesis of cyclic enones via direct palladium-catalyzed aerobic dehydrogenation of ketones, *J. Am. Chem. Soc.*, 2011, **133**, 14566–14569.
55 D. Lorenzo, A. Romero, L. Del-Arco and A. Santos, Transformation of cyclic ketones as impurities in cyclohexanone in the caprolactam production process, *Ind. Eng. Chem. Res.*, 2019, **58**, 21983–21995.
56 J. Gascon, A. Corma, F. Kapteijn and F. X. Llabres i Xamena, Metal Organic Framework catalysis: quo vadis?, *ACS Catal.*, 2014, **4**, 361–378.
57 C. Schotten, T. P. Nicholls, R. A. Bourne, N. Kapur, B. N. Nguyen and C. E. Willans, Making electrochemistry easily accessible to the synthetic chemist, *Green Chem.*, 2020, **22**, 3358–3375.
58 B. A. Frontana-Uribe, R. D. Little, J. G. Ibanez, A. Palma and R. Vasquez-Medrano, Organic electrosynthesis: a promising green methodology in organic chemistry, *Green Chem.*, 2010, **12**, 2099–2119.
59 T. R. Cook, D. K. Dogutan, S. Y. Reece, Y. Surendranath, T. S. Teets and D. G. Nocera, Solar energy supply and storage for the legacy and nonlegacy worlds, *Chem. Rev.*, 2010, **110**, 6474–6502.
60 L. Zhang, J. Xiao, H. Wang and M. Shao, Carbon-based electrocatalysts for hydrogen and oxygen evolution reactions, *ACS Catal.*, 2017, **7**, 7855–7865.
61 P. P. Lopes, D. Tripkovic, P. F. B. D. Martins, D. Strmcnik, E. A. Ticianelli, V. R. Stamenkovic and N. M. Markovic, Dynamics of electrochemical Pt dissolution at atomic and molecular levels, *J. Electroanal. Chem.*, 2018, **819**, 123–129.
62 P. Engels, F. Cerdas, T. Dettmer, C. Frey, J. Hentschel, C. Herrmann, T. Mirfabrikikar and M. Schueler, Life cycle assessment of natural graphite production for lithium-ion battery anodes based on industrial primary data, *J. Cleaner Prod.*, 2022, **336**, 130474.
63 L. Fan, R. Ma, Q. Zhang, X. Jia and B. Lu, Graphite Anode for a Potassium-Ion Battery with Unprecedented Performance, *Angew. Chem., Int. Ed.*, 2019, **58**, 10500–10505.
64 J. B. Dunn, L. Gaines, J. C. Kelly, C. James and K. G. Gallagher, The significance of Li-ion batteries in electric vehicle life-cycle energy and emissions and recycling's role in its reduction, *Energy Environ. Sci.*, 2015, **8**, 158–168.
65 S. Möhle, M. Zirbes, E. Rodrigo, T. Gieshoff, A. Wiebe and S. R. Waldwogel, Modern Electrochemical Aspects for the Synthesis of Value-Added Organic Products, *Angew. Chem., Int. Ed.*, 2018, **57**, 6018–6041.
66 M. Cossutta, J. McKechnie and S. J. Pickering, A comparative LCA of different graphene production routes, *Green Chem.*, 2017, **19**, 5874–5884.
67 Mineral Commodity Summaries 2021, Geological Survey (USGS) technical report. https://minerals.usgs.gov/minerals/pubs/commodity/ (accessed September 2022).
68 N.-T. Suen, S.-F. Hung, Q. Quan, N. Zhang, Y.-J. Xu and H. M. Chen, Electrocatalysis for the Oxygen Evolution Reaction: Recent Development and Future Perspectives, *Chem. Soc. Rev.*, 2017, **46**, 337–365.
69 F. P. Byrne, S. Jin, G. Paggiola, T. H. M. Petchey, J. H. Clark, T. J. Farmer, A. J. Hunt, C. R. McElroy and J. Sherwood, Tools and techniques for solvent selection: green solvent selection guides, *Sustainable Chem. Processes*, 2016, **4**, 7.
70 U. Sanyal, J. Lopez-Ruiz, A. B. Padmaperuma, J. Holladay and O. Y. Gutierrez, *Org. Process Res. Dev.*, 2018, **22**, 1590–1598.
71 P. J. Tortajada, T. Kärnman, P. Martínez-Pardo, C. Nilsson, H. Holmquist, M. J. Johansson and B. Martín-Matute, Electrochemical Reduction of Alkenes over a Nickel Foam Guided by Life Cycle, Safety and Toxicological Assessments, *ChemRxiv*, 2023, preprint, DOI: 10.26434/chemrxiv-2023-p4q71.